Effect of Spinal Cord Injury on Nonlinear Complexity of Skin Blood Flow Oscillations

Yih-Kuen Jan[1], Fuyuan Liao[1], and Stephanie Burns[2]

[1] University of Oklahoma Health Sciences Center, Department of Rehabilitation Sciences, Oklahoma City, Oklahoma, USA
yjan@ouhsc.edu
[2] Oklahoma City Veterans Affairs Medical Center, Department of Neurology and Rehabilitation, Oklahoma City, Oklahoma, USA

Abstract. This study investigated the effect of spinal cord injury (SCI) on nonlinear complexity of skin blood flow oscillations (BFO). Complexity of the characteristic frequencies embedded in BFO was described by the scaling coefficient derived by detrended fluctuation analysis (DFA) and the range of scaling coefficients derived from multifractal detrended fluctuation analysis (MDFA) in specific scale intervals. 23 subjects were recruited into this study, including 11 people with SCI and 12 healthy controls. Local heating-induced maximal sacral skin blood flow was measured by laser Doppler flowmetry. The results showed that metabolic BFO (0.0095-0.02 Hz) exhibited significantly lower complexity in people with SCI as compared with healthy controls ($p<0.01$) during maximal vasodilation. This study demonstrated that complexity analysis of BFO can provide information of blood flow dynamics beyond traditional spectral analysis.

Keywords: blood flow oscillations, complexity, detrended fluctuation analysis, multifractal detrended fluctuation analysis, spinal cord injury.

1 Introduction

Spinal cord injury (SCI) results in an interruption of the autonomic pathways from the brainstem and hypothalamus to the intermediolateral cell column of the spinal cord [1]. This interruption causes a loss or attenuation of modulation of the spinal autonomic reflexes in response to various stimuli at the level below spinal injury. Inability to increase skin blood flow to reduce tissue ischemia following SCI may increase risk for pressure ulcers [2].

Skin blood flow has been studied using two categories of methods: linear and nonlinear analysis. The linear analysis typically starts with the mean and standard deviation, focusing on Fourier spectral analysis or wavelet analysis. Spectral analysis of laser Doppler flowmetry (LDF) signals has revealed five characteristic frequencies [3, 4]. These characteristic frequencies have been associated with heart beats (0.4-2.0 Hz), respiration (0.15-0.4 Hz), myogenic activity (0.05-0.15 Hz), neurogenic

C. Stephanidis (Ed.): Universal Access in HCI, Part IV, HCII 2011, LNCS 6768, pp. 345–355, 2011.

(0.02-0.05 Hz), and metabolic (0.0095-0.02 Hz) activities, respectively [5]. Generally, the time averaged amplitude or power of the characteristic frequencies are used to evaluate the activities of the underlying mechanisms. However, these characteristic frequencies are not constant, but vary with time [4] (Fig. 1). This feature cannot be characterized by time averaged amplitude or power.

The time-varying feature of the characteristic frequencies of BFO may be described by their structural complexity [6]. This complexity arises from the interaction of structural units and regulatory feedback loops that operate over a wide range of temporal and spatial scales [6]. Research suggests that the output of healthy systems exhibits a type of complex variability, and that such complexity degrades with aging and diseases, reducing the adaptive capabilities of the individual [7-9]. Although the concept of complexity has been elaborated for several decades, the use of complexity for diagnostic and prognostic assessment remains a great challenge. Investigators have applied complexity analysis to evaluate variability in physiological signals, e.g. heart rate [10, 11], gait [12], and BFO [13, 14]. These studies provided evidences of clinical importance and potential use to indentify pathological conditions.

To better understand the role of microvascular dysfunction in pressure ulcers, we have conducted a series of studies examining BFO in response to various causative factors of pressure ulcers [14-18]. In this study, we examined the effect of spinal cord injury on microvascular function by quantifying complexity of BFO in response to local heat.

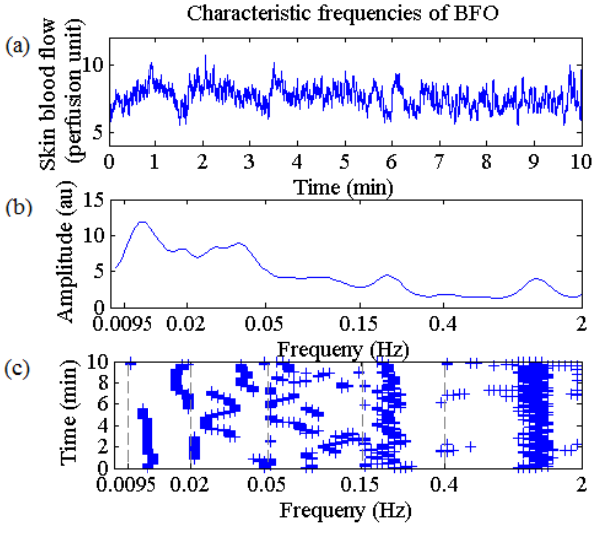

Fig. 1. Characteristic frequencies embedded in BFO. (a) A skin blood flow signal recorded from a healthy subject. (b) The time-averaged amplitudes of the continuous wavelet transform (WT) of the signal. (c) The local maxima of the WT.

2 Methods

2.1 Participants

We recruited 23 subjects into this study, including 11 people with SCI and 12 healthy controls. All subjects with SCI were wheelchair users, with the injury level between C4 and T12, and were at least 6 months post spinal injury. None of the subjects had cardiorespiratory disease, hypertension, or other pathological conditions, and none were taking medications that might affect cardiovascular function or diabetes mellitus. All subjects gave informed consent to this study approved by the University Institutional Review Board. The demographic features of the enrolled subjects are shown in Table 1.

Table 1. Demographic data of the research subjects

	SCI	Healthy controls
Number of subjects	11	12
Gender, M/F	7/4	4/8
Age (years)	35.4(12.4)	25.3 (5.4)
Duration of spinal injury (years)	7.6 (4.9)	-
Body mass index (kg/m^2)	25.1 (4.4)	23.2 (2.4)

Data are expressed as the mean (standard deviation).

2.2 Data Acquisition

After at least a 30 min quiet rest period to become acclimated to the room temperature (24±2˚C), the subject was positioned in a prone posture. Sacral skin blood flow was recorded using the laser Doppler flowmetry (PF 5001, Perimed AB, Sweden) at a sampling frequency of 32 Hz. A heating probe (Probe 415-242, Perimed AB) was used to heat the skin to 42˚C in 2 minutes and to maintain that temperature for 50 min. The protocol included a 10 min pre-heating period, a 50 min heating period, and a 10 min post-heating period [21].

2.3 Complexity Analysis

*Detrended fluctuation analysis (DFA).*The DFA was introduced by Peng et al. [19, 22] to quantify the long-range power law correlations of nonstationary time series. A key issue of the DFA is that the fluctuations driven by extrinsic uncorrelated stimuli are interpreted as a systematic "drift" or "trend," and are treated by removing the least-squares regression in each observation window [23]. To illustrate the DFA algorithm, consider the blood flow signal shown in Figure 1(a). First, the original time series, $\{x(i), i = 1, \dots, N\}$, is integrated after subtracting its mean value

$$y(k) = \sum_{i=1}^{k}(i) - \mu),\ k = 1, \dots, N \tag{1}$$

with μ as the mean of $\{x(i)\}$. The integrated time series is then divided into boxes of equal length, n (Fig. 2(a)). In each box, a least-squares line $y_n(k)$ is fitted to the

integrated series, $\{y(k)\}$. Next, $\{y(k)\}$ is detrended by subtracting the local trend, $y_n(k)$. The root-mean-square fluctuation, $F(n)$, is calculated for all box sizes, n:

$$F(n) = \sqrt{\frac{1}{N}\sum_{k=1}^{N}(y(k) - y_n(k))^2} \tag{2}$$

Finally, $F(n)$ is plotted against n in a log-log scale, and the slope of the regression line gives the scaling exponent, α (Fig. 2(b)). This exponent can be considered as a measure of the "roughness" of the original time series: the larger the value of α, the smoother the time series [8].

The scaling exponent derived by DFA is not always a constant [24], i.e. the log-log plot may exhibit more than one scaling region. A crossover can result from a change in the correlation properties of the signal at different time or space scales [13, 14]. However, a crossover may also arise from the nonstationarities of the signal and/or its trends without any transition in the intrinsic dynamics [25].

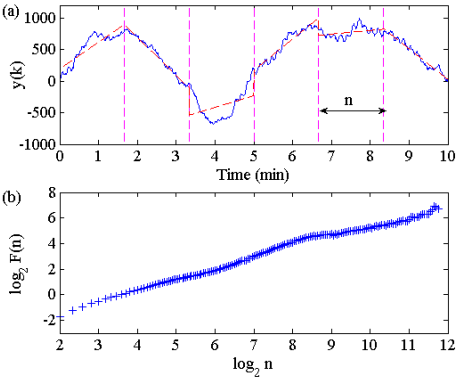

Fig. 2. Illustration of the DFA algorithm. The original time series is the blood flow signal shown in Fig. 1(a). (a) The solid curve is the integrated time series, $y(k)$. The vertical dash lines indicate boxes of size, n. The dashed line segments represent the trend estimated in each box by a linear least squared fit. (b) The deviations, $F(n)$, versus the box size, n, on a log-log scale. There are more than one scaling region.

Multifractal analysis. The DFA algorithm gives only one exponent to characterize a signal. This method, therefore, is most appropriate for the analysis of monofractal signals [8]. Monofractals have the same scaling properties throughout the entire signal. In contrast, for multifractal signals, different parts may have different scaling properties, requiring a large number of indices to characterize their scaling properties. It has been found that heart rate fluctuations exhibit multifractality in healthy human subjects [10, 26]. Moreover, heart rate recorded from patients with heart failure shows a breakdown of multifractality [10]. Recently, a few studies [27, 28] suggested that skin blood flow signals recorded by LDF also have multifractal properties.

The most popular methods for the detection of multifractal scaling properties of a signal are: the wavelet transform modulus maxima (WTMM) [29, 30] and the

multifractal detrended fluctuation analysis (MDFA) [20]. It was suggested that in the case of lacking a priori knowledge of the properties of a process, the MDFA should be recommended [31]. MDFA is a generalization of the standard DFA [20], describing how the q-th order moments of fluctuation depend on the observation scale. For a time series, $\{x(i), i = 1, \ldots, N\}$, defined on a compact support, first, it is integrated after subtracting its mean value. Then the integrated series is divided into m non-overlapping segments of length n and the same procedure is repeated starting from the opposite end ($2m$ segments total). Next, for each segment v, the local trend is estimated by fitting a polynomial and subtracting it from the segment. Let the variance be $F^2(v, n)$, a q-th order fluctuation function is defined as

$$F_q(n) = \begin{cases} \{\frac{1}{2m}\sum_{v=1}^{2m}[F^2(v,n)]^{q/2}\}^{1/q}, & q \neq 0 \\ \exp\{\frac{1}{4m}\sum_{v=1}^{2m}\ln[F^2(v,n)]\}, & q = 0 \end{cases} \tag{3}$$

If the time series is long-range power-law correlated, it is expected that

$$F_q(n) \sim n^{h(q)} \tag{4}$$

Thus one obtains a family of exponents, $h(q)$. For $q = 2$, the standard DFA is retrieved.

The reason for this procedure is that, for positive values of q, $h(q)$ reflects the scaling behavior of the segments with large fluctuations, whereas for negative values of q, $h(q)$ reflects the scaling behavior of the segments with small fluctuations [20]. Thus, for a given signal, if the scaling behavior is identical for all segments, $h(q)$ is independent of q; if small and large fluctuations scale differently, there will be a significant dependence of $h(q)$ on q. For instance, in the scale range of n=1600~3368 (given the sampling frequency 32 Hz, this range is related to the frequency band 0.0095~0.02 Hz, see the following section), $h(q)$ decreases with q, indicating the existence of multifractal scaling behavior of BFO (Fig. 3).

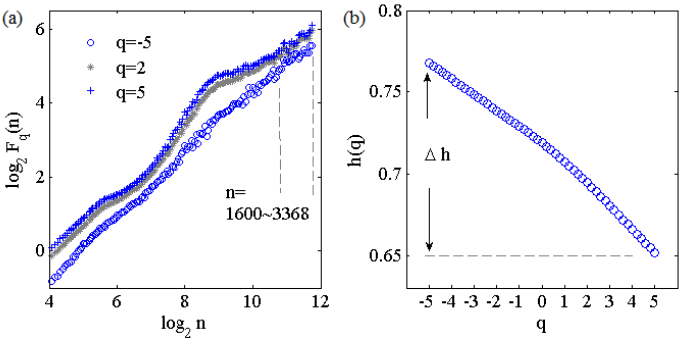

Fig. 3. Illustration of the multifractal detrended fluctuation analysis (MDFA) method. (a) The q-th order fluctuations versus observation scales on a log-log scale, showing different scaling behaviors for different values of q (-5, 2, 5). (b) Scaling exponent in the scale range of n=1600~3368 decreases with q.

2.4 Relationship between Scale (Box Size) and Frequency in DFA (MDFA)

Previous studies have demonstrated that DFA is closely related to power spectral density analysis [32, 33]. Suppose that the power spectral density (PSD) of the original time series, $\{x(i)\}$, is $P_x(\omega)$. The PSD of the integrated series (Eq. (1)), y, is then given by [32]

$$P_y(\omega) = \begin{cases} 0, & \omega = 0 \\ \frac{P_x(\omega)}{2(1-cos\omega)}, & \omega \neq 0 \end{cases} \tag{5}$$

The integrated series, y, is divided into non-overlapping boxes of length n and detrended. It can be numerically verified that the PSD of the detrended series obeys the following relation (Fig. 4)

$$P_y^d \approx \begin{cases} 0, & 0 \leq \omega \leq \omega_s/n \\ P_y(\omega), & otherwise \end{cases} \tag{6}$$

where $\omega_s = 2\pi f_s$ with f_s being the sampling frequency in Hertz. This relation means that detrending in boxes of length n is equivalent to applying a high-pass filter to the integrated series with a cut-off frequency f_s/n. Thus, the scaling behavior of metabolic, neurogenic, and myogenic BFO are respectively characterized by the scaling coefficients in the scale ranges: $f_s/0.02 < s < f_s/0.0095$, $f_s/0.05 < s < f_s/0.02$, and $f_s/0.15 < s < f_s/0.05$.

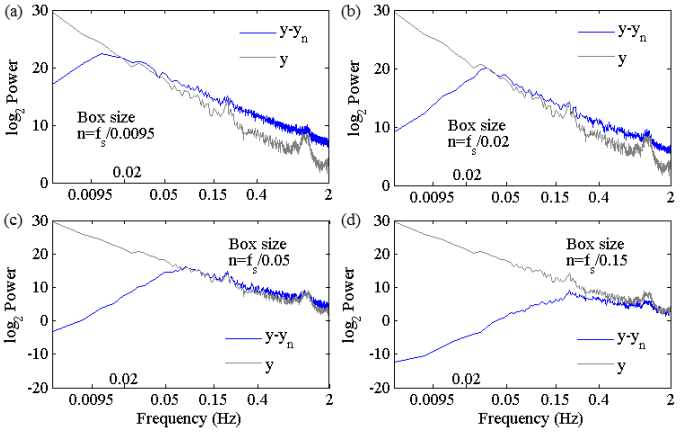

Fig. 4. Relationship between observation scales (box size) and frequencies in DFA and MDFA methods. In all the panels, y denotes the integrated series, $y - y_n$ denotes the detrended series, and n denotes the scale (box size). In the fitting procedure, quadratic polynomials were used. Detrending in boxes of length n is equivalent to applying a high-pass filter to the integrated series with a cut-off frequency f_s/n.

We used $\Delta h = \max(h(q)) - \min(h(q))$ in the scale interval $f_s/0.02 < s < f_s/0.0095$ to quantify the complexity degree of metabolic BFO, the scale interval

$f_s/0.05 < s < f_s/0.02$ to quantify the complexity degree of neurogenic BFO, and scale interval $f_s/0.15 < s < f_s/0.05$ to quantify the complexity degree of myogenic BFO. Comparisons between two groups in the same thermal condition were performed using the Wilcoxon rank sum tests. Comparisons between two thermal conditions in the same group were performed using the Wilcoxon signed rank tests. The significance level was set at p value less than 0.05.

3 Results and Discussion

Fig. 5 shows the DFA coefficient and complexity degree of metabolic oscillations. At baseline, the DFA coefficient showed significantly higher values in healthy controls (p<0.05). However, it did not show significant change either in healthy controls or in people with SCI due to local heating. Unlike DFA coefficient, the complexity degree of metabolic oscillations significantly increased in healthy controls in response to local heating (p <0.01), while not in people with SCI. During the maximal vasodilation, a significant lower degree of complexity was observed in people with SCI (p <0.01). For neurogenic and myogenic BFO, neither DFA coefficient nor complexity degree showed significant differences between healthy controls and people with SCI.

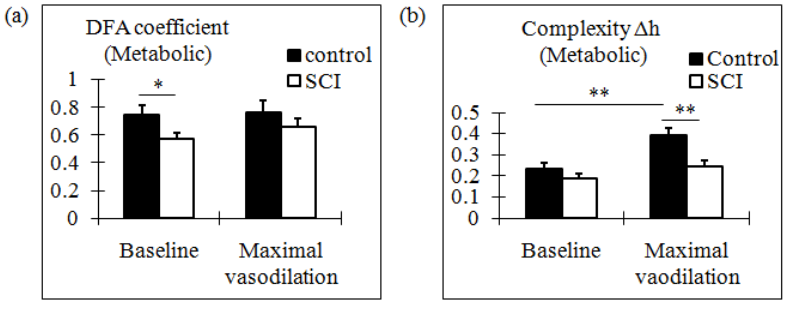

Fig. 5. Comparisons of DFA coefficient and complexity degree of metabolic oscillations between healthy controls and people with SCI. Values are expressed as means ± SE. * indicates p<0.05; ** indicates p<0.01.

We have shown that people with SCI had a lower complex behavior of metabolic oscillations. From our results, we may deduce that metabolic oscillations in healthy people have richer structures than in people with SCI. Our results support the concept that decreased complexity of a physiologic process is associated with pathological states [6, 7]. Previous studies have demonstrated that attenuated metabolic and neurogenic oscillations are associated with vasodilatory dysfunction [18]. Li et al. [34] observed a lower amplitude of metabolic frequency in people with SCI as compared with healthy controls. However, the dynamics of skin blood flow or of a characteristic frequency contain not only the amplitude, but also the variations in frequency and amplitude. The latter cannot be characterized by time-averaged

amplitude or power. Although wavelet based time-frequency-amplitude presentation can describe how frequency and amplitude change with time, difficulties may arise from quantifying the changes [18].

Fig. 6 compares the dynamics of metabolic oscillations in a healthy subject with those in a subject with SCI. The blood flow signal shown in Fig. 1(a) and a blood flow signal recorded from a subject with SCI have almost the same time-averaged amplitude of WT in the frequency band, 0.0095-0.02 Hz. However, by comparing the time-frequency-amplitude presentations (Fig.6 (a) and (b)), it can be seen that the metabolic frequency in the healthy subject appears to have more complex behavior. This visual intuition can be verified by the MDFA. As shown in Fig. 6 (c) and (d), the metabolic frequency in the healthy subject has a wider range of scaling exponents, i.e., more complex dynamics.

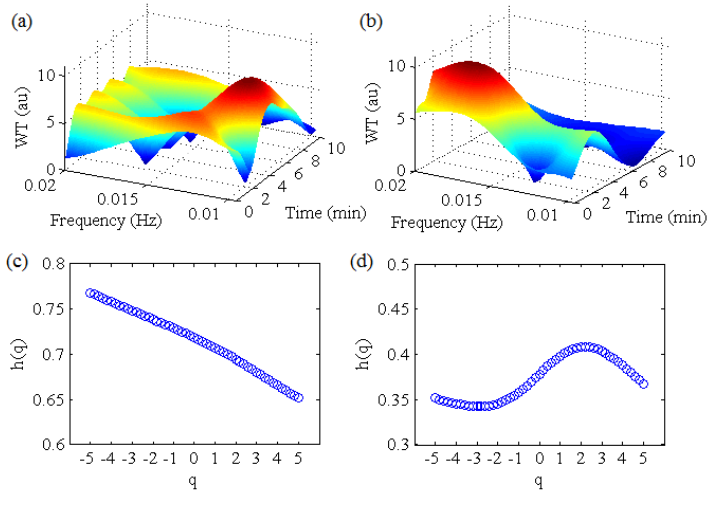

Fig. 6. Comparisons of the dynamics of metabolic frequency between a healthy subject and a subject with SCI. (a) Continuous wavelet transform (WT) of a blood flow signal in health (0.0095-0.02 Hz). (b) WT of a blood flow signal in SCI (0.0095-0.02 Hz). (c) MDFA of the blood flow signal in health (0.0095-0.02 Hz). (d) MDFA of the blood flow signal in SCI (0.0095-0.02 Hz).

4 Conclusion

Our results provided evidence that people with SCI have altered dynamics of skin blood flow: metabolic frequency of BFO in people with SCI exhibits less complexity compared to that in healthy people. Complexity analysis of BFO can provide information on blood flow dynamics beyond linear analysis, which might be used to study the interactions among blood flow control mechanisms in various pathological conditions.

Acknowledgements. This work was supported by the National Institutes of Health (R03HD060751) and the Christopher and Dana Reeve Foundation (JA2-0701-2).

References

1. Alexander, M.S., Biering-Sorensen, F., Bodner, D., Brackett, N.L., Cardenas, D., Charlifue, S., et al.: International standards to document remaining autonomic function after spinal cord injury. Spinal Cord 47(1), 36–43 (2009)
2. Nixon, J., Cranny, G., Bond, S.: Pathology, diagnosis, and classification of pressure ulcers: comparing clinical and imaging techniques. Wound Repair Regen 13(4), 365–372 (2005)
3. Stefanovska, A., Bracic, M., Kvernmo, H.D.: Wavelet analysis of oscillations in the peripheral blood circulation measured by laser Doppler technique. IEEE Trans. Biomed. Eng. 46(10), 1230–1239 (1999)
4. Bracic, M., Stefanovska, A.: Wavelet-based analysis of human blood-flow dynamics. Bull. Math. Biol. 60(5), 919–935 (1998)
5. Stefanovska, A., Bracic, M.: Physics of the human cardiovascular system. Contemporary Physics 40(1), 31–55 (1999)
6. Goldberger, A.L., Peng, C.K., Lipsitz, L.A.: What is physiologic complexity and how does it change with aging and disease? Neurobiology of Aging 23(1), 23–26 (2002)
7. Lipsitz, L.A., Goldberger, A.L.: Loss of Complexity and Aging - Potential Applications of Fractals and Chaos Theory to Senescence. Jama-Journal of the American Medical Association 267(13), 1806–1809 (1992)
8. Goldberger, A.L., Amaral, L.A.N., Hausdorff, J.M., Ivanov, P.C., Peng, C.K., Stanley, H.E.: Fractal dynamics in physiology: Alterations with disease and aging. Proceedings of the National Academy of Sciences of the United States of America 99, 2466–2472 (2002)
9. Goldberger, A.: Complexity loss, aging, and disease: Is there a dynamical "Theory of Everything Pathologic?". Journal of Critical Care 25(3), E2 (2010)
10. Ivanov, P.C., Amaral, L.A.N., Goldberger, A.L., Havlin, S., Rosenblum, M.G., Struzik, Z.R., et al.: Multifractality in human heartbeat dynamics. Nature 399(6735), 461–465 (1999)
11. Merati, G., Di Rienzo, M., Parati, G., Veicsteinas, A., Castiglioni, P.: Assessment of the autonomic control of heart rate variability in healthy and spinal-cord injured subjects: contribution of different complexity-based estimators. IEEE Trans. Biomed. Eng. 53(1), 43–52 (2006)
12. Harbourne, R.T., Stergiou, N.: Movement Variability and the Use of Nonlinear Tools: Principles to Guide Physical Therapist Practice Response. Physical Therapy 89(3), 284–285 (2009)
13. Esen, F., Esen, H.: Detrended fluctuation analysis of laser Doppler flowmetry time series: the effect of extrinsic and intrinsic factors on the fractal scaling of microvascular blood flow. Physiological Measurement 27(11), 1241–1253 (2006)
14. Liao, F., Garrison, D.W., Jan, Y.K.: Relationship between nonlinear properties of sacral skin blood flow oscillations and vasodilatory function in people at risk for pressure ulcers. Microvasc Res. 80(1), 44–53 (2010)
15. Geyer, M.J., Jan, Y.K., Brienza, D.M., Boninger, M.L.: Using wavelet analysis to characterize the thermoregulatory mechanisms of sacral skin blood flow. Journal of Rehabilitation Research and Development 41(6A), 797–805 (2004)

16. Jan, Y.K., Brienza, D.M., Geyer, M.J.: Analysis of week-to-week variability in skin blood flow measurements using wavelet transforms. Clin. Physiol. Funct. Imaging 25(5), 253–262 (2005)
17. Jan, Y.K., Brienza, D.M., Geyer, M.J., Karg, P.: Wavelet-based spectrum analysis of sacral skin blood flow response to alternating pressure. Arch. Phys. Med. Rehabil. 89(1), 137–145 (2008)
18. Jan, Y.K., Struck, B.D., Foreman, R.D., Robinson, C.: Wavelet analysis of sacral skin blood flow oscillations to assess soft tissue viability in older adults. Microvasc. Res. 78(2), 162–168 (2009)
19. Peng, C.K., Buldyrev, S.V., Havlin, S., Simons, M., Stanley, H.E., Goldberger, A.L.: Mosaic Organization of DNA Nucleotides. Physical Review E 49(2), 1685–1689 (1994)
20. Kantelhardt, J.W., Zschiegner, S.A., Koscielny-Bunde, E., Havlin, S., Bunde, A., Stanley, H.E.: Multifractal detrended fluctuation analysis of nonstationary time series. Physica a-Statistical Mechanics and Its Applications 316(1-4), 87–114 (2002)
21. Minson, C.T., Berry, L.T., Joyner, M.J.: Nitric oxide and neurally mediated regulation of skin blood flow during local heating. Journal of Applied Physiology 91(4), 1619–1626 (2001)
22. Peng, C.K., Havlin, S., Hausdorff, J.M., Mietus, J.E., Stanley, H.E., Goldberger, A.L.: Fractal mechanisms and heart rate dynamics - Long-range correlations and their breakdown with disease. Journal of Electrocardiology 28, 59–65 (1995)
23. Meyer, M., Stiedl, O.: Self-affine fractal variability of human heartbeat interval dynamics in health and disease. Eur. J. Appl. Physiol. 90(3-4), 305–316 (2003)
24. Chen, Z., Ivanov, P., Hu, K., Stanley, H.E.: Effect of nonstationarities on detrended fluctuation analysis. Phys. Rev. E Stat. Nonlin. Soft. Matter Phys. 65(4 Pt 1), 041107 (2002)
25. Hu, K., Ivanov, P.C., Chen, Z., Carpena, P., Stanley, H.E.: Effect of trends on detrended fluctuation analysis. Physical Review E 6401(1) (2001)
26. Havlin, S., Amaral, L.A., Ashkenazy, Y., Goldberger, A.L., Ivanov, P., Peng, C.K., et al.: Application of statistical physics to heartbeat diagnosis. Physica a-Statistical Mechanics and Its Applications 274(1-2), 99–110 (1999)
27. Humeau, A., Chapeau-Blondeau, F., Rousseau, D., Rousseau, P., Trzepizur, W., Abraham, P.: Multifractality, sample entropy, and wavelet analyses for age-related changes in the peripheral cardiovascular system: Preliminary results. Medical Physics 35(2), 717–723 (2008)
28. Humeau, A., Chapeau-Blondeau, F., Rousseau, D., Tartas, M., Fromy, B., Abraham, P.: Multifractality in the peripheral cardiovascular system from pointwise holder exponents of laser Doppler flowmetry signals. Biophysical Journal 93(12), L59–L61 (2007)
29. Arneodo, A., Bacry, E., Muzy, J.F.: The Thermodynamics of Fractals Revisited with Wavelets. Physica a-Statistical Mechanics and Its Applications 213(1-2), 232–275 (1995)
30. Bacry, E., Muzy, J.F., Arneodo, A.: Singularity Spectrum of Fractal Signals from Wavelet Analysis - Exact Results. Journal of Statistical Physics 70(3-4), 635–674 (1993)
31. Oswiecimka, P., Kwapien, J., Drozdz, S.: Wavelet versus detrended fluctuation analysis of multifractal structures. Phys. Rev. E Stat. Nonlin. Soft. Matter Phys. 74(1 Pt 2), 016103 (2006)
32. Heneghan, C., McDarby, G.: Establishing the relation between detrended fluctuation analysis and power spectral density analysis for stochastic processes. Physical Review E 62(5), 6103–6110 (2000)

33. Willson, K., Francis, D.P., Wensel, R., Coats, A.J.S., Parker, K.H.: Relationship between detrended fluctuation analysis and spectral analysis of heart-rate variability. Physiological Measurement 23(2), 385–401 (2002)
34. Li, Z., Leung, J.Y., Tam, E.W., Mak, A.F.: Wavelet analysis of skin blood oscillations in persons with spinal cord injury and able-bodied subjects. Arch. Phys. Med. Rehabil. 87(9), 1207–1212 (2006), quiz 1287